Scattering properties of the triangnlar Ising antiferromagnet: Disorder and Lifshitz lines

T. Garel
Service de Physique Théorique, Centre d'Études Nucléaires de Saclay, 91191 Gif-sur-Yvette Cedex, France

V. Ilakovac* and S. Ravy
Laboratoire de Physique des Solides, Bâtiment 510, Université Paris-Sud, 91405 Orsay, France
(Received 30 November 1993)

We study an anisotropic nearest-neighbor Ising antiferromagnet on the triangular lattice, using Monte-Carlo simulations and random-phase (or related) approximations. Our main interest concerns the high-temperature magnetic scattering. Exact results are available at the disorder line (Stephenson; Welberry and Galbraith). Of greater experimental significance is the Lifshitz line where (i) splitting of the scattering peaks occurs and (ii) dislocationlike defects appear in the (instantaneous) spin configurations. A good analytical fit of the Lifshitz line is given by the Bethe-Peierls approximation. These results could be relevant to other systems with disorder lines, e.g., the *ANNNI* model and microemulsions.

I. INTRODUCTION

Systems with competing interactions may exhibit various types of fluctuations in their disordered phases. Of particular interest are systems possessing a disorder point[1] (or line in a more general phase diagram) where the nature of the short-range order changes (e.g., from oscillatory to nonoscillatory). Experimental systems in this class include microemulsions,[2] liquid crystals,[3] antiferromagnetic in a field,[4] etc. Scattering experiments on these materials display non-Ornstein-Zernike (OZ) behavior at high temperature: roughly speaking, one must add a "q^4" term to the denominator of the traditional OZ form[5] to fit the experimental data.

Recently,[6] we have performed x-ray diffuse scattering experiments on the organic compounds $(TMP)_2X-CH_2Cl_2$, where TMP is 3,4,9-10 tetramethylperylene, X a PF_6^- or AsF_6^- anion and CH_2Cl_2 a solvent molecules. In this compound, long-range-ordered chains of alternating anion-solvent (A/S) molecules can occupy two positions in the channels between the stacks of organic molecules. The transverse correlations between the (A/S) chains positions have been first investigated by x-ray diffuse scattering experiments at ambient temperature. If one represents[6] the positions of the chains by an Ising spin variable, the transverse correlations between the chains can be modeled by the anisotropic triangular antiferromagnet,[7] with nearest-neighbor (or next-nearest-neighbor) interactions. This model has a disorder point in the high-temperature phase. Moreover, the x-ray scattering experiments[6] exhibit unexpected features.

In this paper, following Stephenson's random-phase approximation (RPA),[8] we explore the scattering properties of the anisotropic triangular antiferromagnet in the disordered phase. To be beyond the RPA, we perform Monte Carlo (MC) simulations with emphasis on both disorder (T_D) and Lifshitz (T_L) points or lines. This latter point may be roughly defined[9] by the temperature at which the "q^2" term in the denominator of the OZ form vanishes or equivalently by the temperature at which the oscillatory character of the fluctuations (appearing at T_D) is large enough to induce a shift of the position of the intensity maxima. The setout of the paper is as follows. The model is defined in Sec. II, where some crystallographic notations are also established. Section III is a rapid summary of RPA and exact results (see also the Appendix). The results of the MC simulations, such as the determination of T_L are given in Sec. IV. We show, in particular, that some features of the high-temperature scattering is well accounted for by the Bethe-Peierls approximation. We finally conclude by some remarks on the appearance of new spin defects, as one crosses T_L.

II. DEFINITIONS AND NOTATIONS OF THE ANISOTROPIC ISING MODEL

We consider [Fig. 1(a)] a triangular lattice with unit basis vector $\mathbf{A}$ and $\mathbf{B}$. At each site $\mathbf{r}=u\,\mathbf{A}+v\mathbf{B}$ [$\equiv(u,v)u,v$ integers] of the lattice we consider an Ising variable $S_{u,v}=\pm1$, interacting with its six nearest neighbors at sites $(u\pm1,v)$, $(u,v\pm1)$, and $(u,v)\pm(1,1)$. The antiferromagnetic interactions along $\mathbf{A},\mathbf{B}$ and $\mathbf{A}+\mathbf{B}$ are, respectively, $J_1,J_2=J_1$ and J_3. In the following we will also use the variables $K_i=\beta J_i (i=1,3)$, and $v_i=\mathrm{th}(K_i)$, where β is the inverse temperature ($\beta=1/k_BT$). The first Brillouin zone is shown in Fig. 1(b). If A^* and B^* denote the basis vectors of the reciprocal lattice (defined by $\mathbf{A}.\mathbf{A}^*=2\pi$, $\mathbf{B}.\mathbf{B}^*=2\pi$, $\mathbf{A}.\mathbf{B}^*=\mathbf{B}.\mathbf{A}^*=0$), one has $\Gamma M=(\mathbf{A}^*-\mathbf{B}^*)/2$, $\Gamma K=(2\mathbf{A}^*-\mathbf{B}^*)/3$, $\Gamma E=(3\mathbf{A}^*-B^*)/4$, etc., to mention a few points of interest. Let us note that in the case $J_1=J_2$, the lattice can be described by an $(\mathbf{a},\mathbf{b})$ centered rectangular cell, also shown in Fig. 1(a).

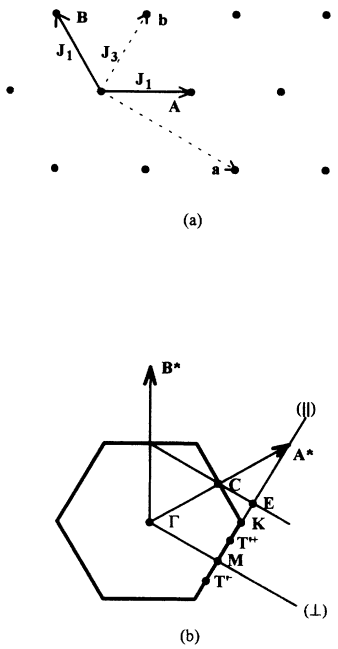

FIG. 1. (a) Definition of the parameters of the model. (b) The first Brillouin zone. Note that the system has a mirror symmetry with respect to ΓM.

III. SUMMARY OF RPA AND EXACT RESULTS

A. RPA results

In the high-temperature phase, the scattered intensity at the wave vector $\mathbf{q}=h\,\mathbf{A}^*+k\mathbf{B}^*$ is proportional[5] to the wave-vector-dependent static susceptibility $\chi(\mathbf{q})$. The RPA result is

$$\chi(\mathbf{q})=\frac{1}{1-\beta J(\mathbf{q})}\ , \tag{1}$$

where

$$\mathbf{J}(\mathbf{q})=2J_1\cos(2\pi h)+2J_1\cos(2\pi k)+2J_3\cos[2\pi(h+k)]\ . \tag{2}$$

For $|J_3/J_1|\cong 0$, the intensity maximum is around the M point (see the Appendix). It turns out that the RPA phase diagram[8] can be easily obtained by studying the vicinity of point M [Fig. 1(b)]. Along the longitudinal ($\|$) $\mathbf{A}^*+\mathbf{B}^*$ direction, we define

$$\mathbf{q}_\|=(\mathbf{A}^*-\mathbf{B}^*)/2\pm\delta_\|(\mathbf{A}^*+\mathbf{B}^*)/2\ , \tag{3a}$$

corresponding to points $T'^{\pm}$ of Fig. 1(b) and along the transverse ($\perp$) $\mathbf{A}^*-\mathbf{B}^*$ direction

$$\mathbf{q}_\perp=(\mathbf{A}^*-\mathbf{B}^*)/2\pm\delta_\perp(\mathbf{A}^*-\mathbf{B}^*)/2\ . \tag{3b}$$

The profile of intensity along the ($\|$) direction is given by

$$\chi(\mathbf{q}_\|)=\frac{1}{(1-2|K_3|-K_1^2/|K_3|)+4|K_3|(\cos\pi\delta_\|-K_1/2K_3)^2}\ , \tag{4}$$

and along the transverse ($\perp$) direction

$$\chi(\mathbf{q}_\perp)=\frac{1}{1+2|K_3|-4|K_1|\cos\pi\delta_\perp}\ . \tag{5}$$

From Eq. (4), we find that (i) the disorder temperature T_D^{RPA} is given[8] by

$$1-2|K_3|-\frac{K_1^2}{|K_3|}=0\ , \tag{6}$$

which can be compared with the exact result [Eq. (A2)]. Let us remark that for thin enough peaks, the intensity has thus a squared Lorentzian shape in the ($\|$) direction. (ii) The Lifshitz line is given by $K_1/2K_3=J_1/2J_3=1$, which is independent of the temperature. For thin enough peaks the usual $1/(C^{\mathrm{st}}+\delta_\|^4)$ form is recovered in the ($\|$) direction.

As a result, for $-\frac{1}{2}<J_3/|J_1|<0$ the high-temperature scattering is maximum at the M point ($\delta_\|=0$, $\delta_\perp=0$) above and below the disordered point and for $J_3/|J_1|<-\frac{1}{2}$ the maximum is at points $T'^{\pm}$

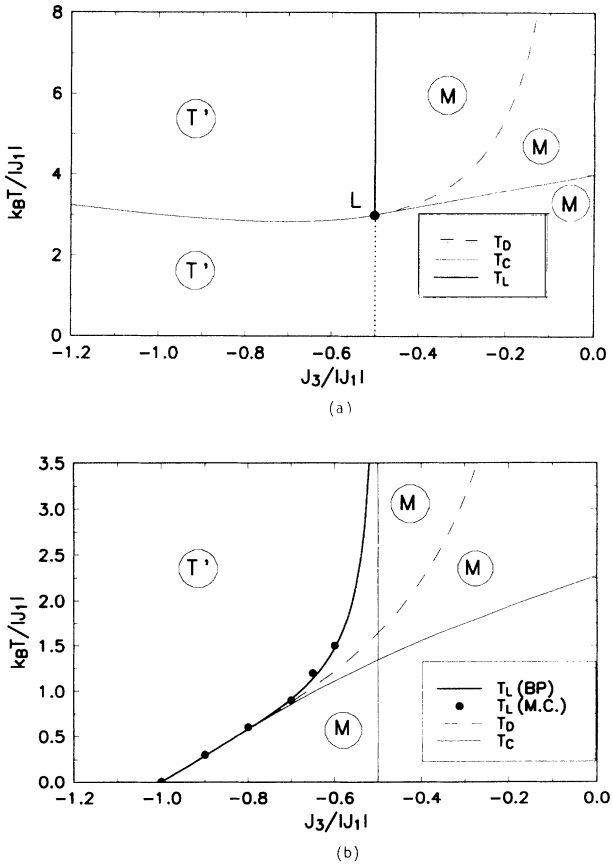

FIG. 2. (a) RPA phase diagram. The circled letters indicate the points of maximal scattered intensity obtained from $\delta_\|=1/\pi a\cos(J_1/2J_3)$. Below T_c are the possible (and unreliable) ordered phases. (b) "Exact" phase diagram. The Lifshitz line comes from the MC simulations. The circled letters indicate the points of maximal scattered intensity. Note that $T_c=0$ for $J_3/|J_1|<-1$ and that the scattering is around point K for $J_3/|J_1|=-1$ at all temperatures.

$[\delta_{\parallel}=(1/\pi)a\cos(J_1/2J_3)$, $\delta_{\perp}=0]$. As the position of the $T'^{\pm}$ points does not depend on the temperature, the splitting of the scattering occurs by crossing the vertical $J_1=2J_3$ line. This splitting was called "anomalous scattering" in Ref. 8.

The full RPA phase diagram is shown in Fig. 2(a) with possible, but unreliable, ordered phases. Finally, let us note that the RPA approximation may also be applied to non-Ising spins.[10]

B. Exact results

Most of the exact results are summarized in the Appendix. The exact phase diagram is shown in Fig. 2(b). As expected, the RPA approach is qualitatively correct at high temperature. Furthermore, (i) the exact solution[7] shows that the slope of $d\xi_3/dT$ (where ξ_3 is the correlation length in the parallel direction) is discontinuous at T_D [as in RPA (Ref. 11)], that is $d\xi_3^+/dT|_{T_D} \neq d\xi_3^-/dT|_{T_D}$. (ii) The exact result[12] on the scattered intensity, at T_D [see Eq. (A6)], yields for $\mathbf{q}=\mathbf{q}_{\parallel}$

$$\chi(\mathbf{q}_{\parallel})=\frac{1}{(1-2|\gamma|\cos\pi\delta_{\parallel})^2}\ , \tag{7}$$

with $\gamma=v_1/(1+v_1^2)$, which gives a perfect square RPA-like form (4). As far as the transverse direction is concerned, an intensity profile similar to (5) is also recovered, namely,

$$\chi(\mathbf{q}_{\perp})=\frac{1}{1+4|\gamma|^2-4|\gamma|\cos\pi\delta_{\perp}}\ . \tag{8}$$

Let us now consider the MC determination of the Lifshitz line, which was already observed in some crystal growth simulations.[13]

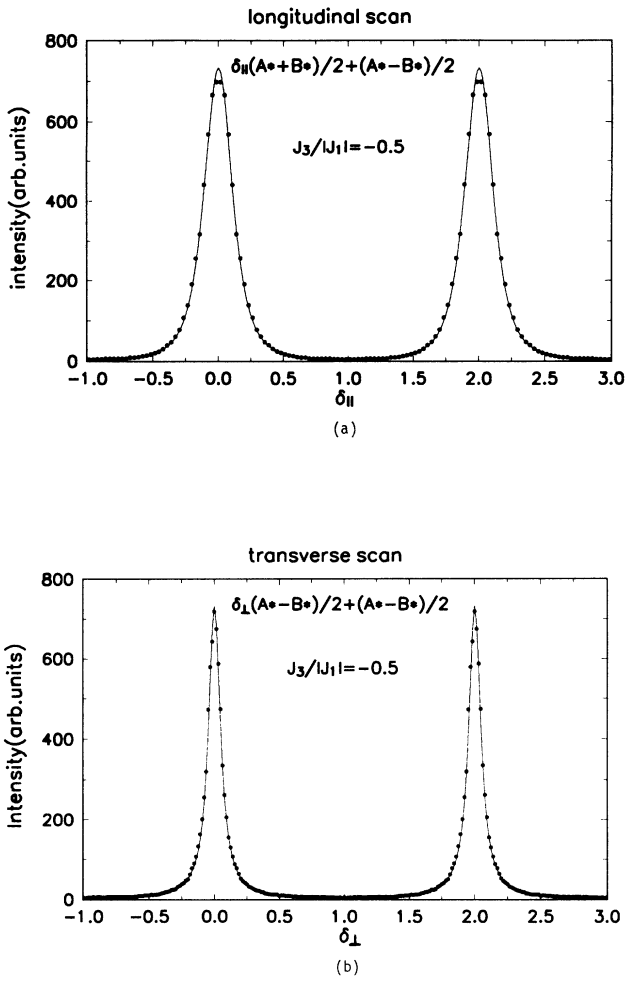

FIG. 3. Fit of MC calculations by the exact forms (7) and (8) at T_D for $J_3/|J_1|=-0.5$. (a) Scattered intensity profile along the ($\parallel$) direction. (b) Scattered intensity profile along the ($\perp$) direction.

IV. MONTE CARLO SIMULATIONS

A. Simulation procedure

We have simulated the model of Fig. 1(a) on a centered rectangular lattice of 1024*1024(**a**,**b**) cells with cyclic boundary conditions. The spins were updated in a sequential way. Since we are not interested in critical phenomena, we only performed 256 Monte Carlo steps/spin (MCS), which was enough achieve thermal equilibrium. We then calculate

$$\chi(\mathbf{q})=\left|\sum_{u,v}S_{u,v}e^{i\mathbf{q}\cdot\mathbf{r}}\right|^2\ , \tag{9}$$

by a fast Fourier transform. The resulting intensity was smoothed by averaging $\chi(\mathbf{q})$ over 4*4 neighbor pixels to obtain the scattering intensity in 131.072 points of the first Brillouin zone. This procedure is equivalent to average the intensity over 16(256**a***256**b**) subsystems. It is expected to be correct for reduced correlation lengths smaller than $\cong 256$, which assures the independence of the subsystems.

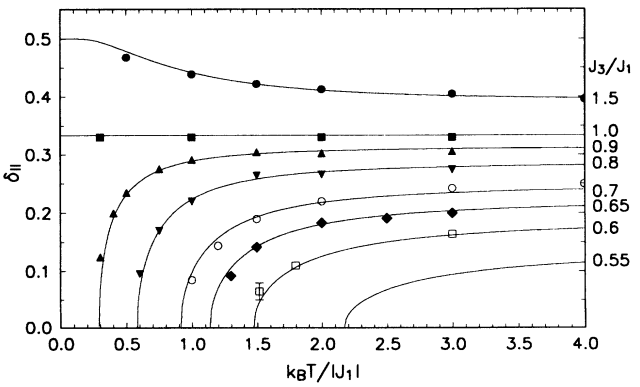

FIG. 4. Temperature dependence of $\delta_{\parallel}$ above the Lifshitz line for different $J_3/|J_1|$ values obtained by MC simulations. The solid lines are the Bethe-Peierls $\delta_{\parallel}(T)$ curves for the same $J_3/|J_1|$ values.

B. Intensity fits at $T=T_D$

We have first checked our Monte Carlo procedure by fitting the intensity profiles obtained at the disorder point with the exact expressions (7) and (8) with no adjustable parameters. As displayed in Fig. 3 for $J_3/|J_1|=-0.5$ ($T_D/|J_1|=1.641$), the agreement is excellent for both longitudinal and transverse scans. We have then tried to find the kink in the derivative $d\xi/dT$ at $T=T_D$ (where ξ is a typical correlation length). We adopted an empirical approach by plotting the longitudinal inverse half width at half maximum (HWHM) in function of T. The result is not very conclusive. Moreover, fitting the longitudinal intensity profiles by a squared Lorentzian does not yield accurate value of T_D either. We thus conclude from this study that disorder points (of the first kind) are quite difficult to characterize experimentally, at least in a static way.[14]

C. Fits of the Lifshitz line

In our simulations, we do observe a Lifshitz line for $-1<J_3/|J_1|<-\frac{1}{2}$, where the maximum of the scattered intensity shifts from point M to points $T'^{\pm}$ at wave vectors

$$\mathbf{q}_{\parallel}=(\mathbf{A}^*-\mathbf{B}^*)/2\pm\delta_{\parallel}(\mathbf{A}^*+\mathbf{B}^*)/2 .$$

The distance $T'^{+}T'^{-}=\delta_{\parallel}$ was found to vary with temperature, for $J_3/|J_1|$ fixed (Fig. 4), in marked contrast to the RPA results (Sec. III A). We tried various analytical fits of $\delta_{\parallel}(T)$: the best turns out to be the Bethe-Peierls (BP) approximation,[15] even though it yields an inaccurate value of the disorder temperature and incorrect shape of the intensity profiles. The wave-vector-dependent susceptibility reads, in the BP approximation,

$$\chi_{\mathrm{BP}}(\mathbf{q})=\left[1+\frac{4v_1^2}{1-v_1^2}+\frac{2v_3^2}{1-v_3^2}-\frac{2v_1}{1-v_1^2}(\cos 2\pi h+\cos 2\pi k)-\frac{2v_3}{1-v_3^2}\cos 2\pi(h+k)\right]^{-1} . \tag{10}$$

Equation (10) yields, for the Lifshitz line,

$$\sinh\left[\frac{2J_1}{T_L}\right]=2\sinh\left[\frac{2J_3}{T_L}\right] , \tag{11a}$$

and the splitting $\delta_{\parallel}$

$$\cos\pi\delta_{\parallel}=\frac{v_2}{2v_3}\frac{1-v_3^2}{1-v_1^2} . \tag{11b}$$

The Lifshitz line is shown in Fig. 2(b), together with the results of the numerical simulation. The variations of $\delta_{\parallel}$ with the temperature given by (11b) are shown in Fig. 4 for various values of $J_3/|J_1|$ including values smaller than -1. For $J_3/|J_1|$ close to -0.5, the Lifshitz temperature is large and the peaks at T'^{+} and T'^{-} are not well separated which makes the estimation of $\delta_{\parallel}$ difficult.

D. Remarks on the defects

For $J_3/|J_1|<-0.5$, the intensity maxima around the points $T'^{\pm}$ implies that the model can be described by an

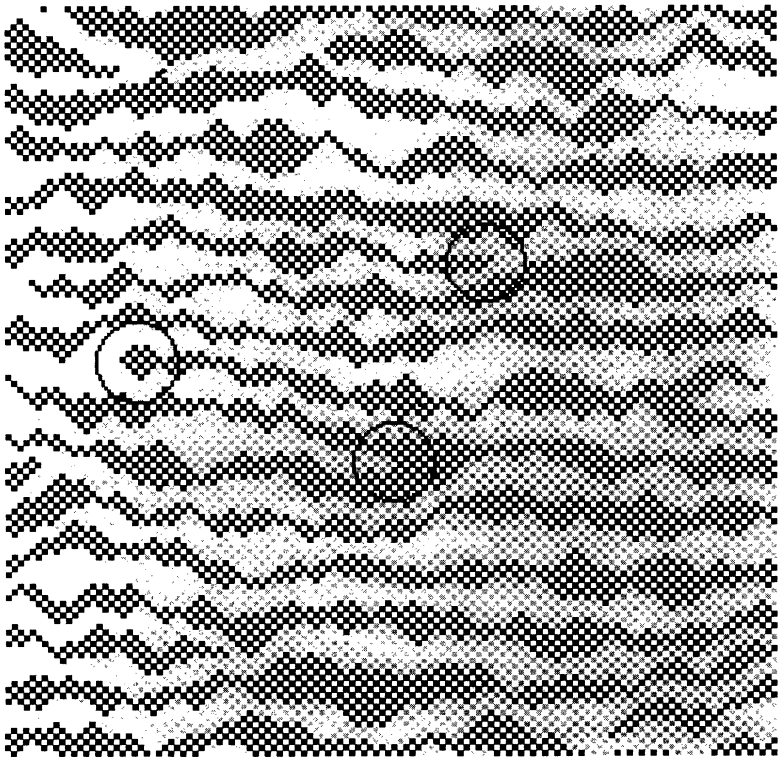

FIG. 5. Snapshot of a (64a*64b) part of the lattice after 256 MCS. Spin $+1$ (-1) are in black (grey). Dislocationlike configurations are clearly visible (circles). Note that the transformation $J_1\rightarrow -J_1$ and $S_{u,v}\rightarrow(-1)^{u+v}S_{u,v}$ has been used in order to make more apparent the ordered domains.

XY model (Ising spins with uniaxial incommensurate modulation) in a way similar to the *ANNNI* model.[16] In particular, we expect to have vortices in our model. In Fig. 5, we show a snapshot corresponding to $J_3/|J_1|=-0.9$ and $T/|J_1|=0.5$ where we have dislocationslike configurations, quite similarly to the *ANNNI* case. It is striking that a disorder line of the first kind may imply the appearance of new defects since, below T_C, we only expect lines to be present.

V. CONCLUSION

We have studied the scattering properties of the anisotropic triangular Ising antiferromagnet by numerical simulations. The existence of a Lifshitz line above the disorder temperature is established for $-1<J_3/|J_1|<-0.5$. This line is well fitted by the Bethe-Peierls approximation. The disorder line itself is found to be hard to characterize in static scattering experiments.[6] Also of interest is the existence of new spin defects (vortices) above T_L. These defects may have a dynamic signature, especially in deep quench experiments: in the related *ANNNI* model, these defects could lead to a glassy phase as observed in numerical simulations.[17]

ACKNOWLEDGMENTS

We thank D. Petermann for writing the data analysis. Laboratoire de Physique des Solides in Unité de Recherche Associée an CNRS No. 2.

APPENDIX: SOME EXACT RESULTS

The model of Fig. 1(a) was solved by Stephenson.[7] The critical temperature T_c is defined by

$$z_1^2-2z_1z_3=1\ , \tag{A1}$$

where $z_i=e^{-2K_i}$ (note that the critical temperature is zero for $J_3/|J_1|<-1$). Below T_c, long-range order sets in, the weak J_3 bond being frustrated. Above T_c, the corresponding fluctuations give a scattering peak at point M [Fig. 1(b)]. Above T_D, defined by

$$z_1^2-2z_1z_3=-1 \tag{A2}$$

(or equivalently by $v_3+v_1^2=0$), the nature of the short-range order changes. Taking as an example the correlation function along the (1,1), direction of the lattice, we have

$$T>T_D:\ w(m,m)\equiv\langle S_{0,0}S_{m,m}\rangle \cong(-1)^m C_+(T)\frac{e^{-|m|/\xi_3^+(T)}}{\sqrt{|m|}} \times\cos[m\theta_3(T)+\Psi_3(T)]\ , \tag{A3}$$

$$T=T_D:\ w(m,m)=|v_3|^m\ , \tag{A4}$$

$$T_c<T<T_D:\ w(m,m)\cong C_-(T)\frac{e^{-|m|/\xi_3^-(T)}}{\sqrt{|m|}}\ , \tag{A5}$$

where the large-m limit is assumed. The temperature dependence of $C_\pm(T)$, $\xi_3^\pm(T)$, $\theta_3(T)$, and $\Psi_3(T)$ are given in Ref. 7. Similar results hold for the (1,0) and (0,1) directions, with subscript 3 replaced by 1.

Above T_L, the maximum intensity peak starts to shift from point M along the ($\|$) direction of Fig. 1(b). This is why we have found more convenient to work with the ($\|$) and the ($\perp$) directions than to use θ_3 (and θ_1) variables. Furthermore, we note that the scattered intensity (i.e., all spin-spin correlation function) is known at T_D as Welberry *et al.* have shown[12] in a crystal growth context. The result is

$$\chi(\mathbf{q})=\frac{1}{1+2\gamma^2+2|\gamma|(\cos2\pi h+\cos2\pi k)+2\gamma^2\cos2\pi(h+k)} \tag{A6}$$

with $\gamma=v_1/(1+v_1^2)$.

*On leave from "Rudjer Boskovic," Bijenica c.54, POB 1016, 41001 Zagreb, Croatia.

[1] J. Stephenson, Can. J. Phys. **47**, 2621 (1969); **48**, 1724 (1970). We will consider in this paper only disorder points of the first kind.

[2] M. Schick, J. Phys. (Paris) Colloq. **4**, C1-47 (1973); K. V. Schuber and R. Strey, J. Chem. Phys. **95**, 8532 (1991).

[3] J. H. Chen and T. C. Lubensky, Phys. Rev. A **14**, 1202 (1976); L. J. Martinez-Miranda, A. R. Kortan, and R. J. Birgeneau, Phys. Rev. Lett. **56**, 2264 (1986).

[4] K. Binder, W. Kinzel, and W. Selke, J. Magn. Magn. Mater. **31-34**, 1445 (1983).

[5] See, e.g., S. W. Lovesey, *Theory of Neutron Scattering from Condensed Matter* (Clarendon, Oxford, 1984).

[6] V. Ilakovac, S. Ravy, A. Moradpour, L. Firlej, and P. Bernier (unpublished).

[7] J. Stephenson, J. Math. Phys. **11**, 420 (1970).

[8] J. Stephenson, Phys. Rev. B **15**, 5442 (1977); **15**, 5453 (1977).

[9] R. M. Hornreich, J. Magn. Magn. Mater. **15-18**, 387 (1980).

[10] H. Kawamura and S. Miyashita, J. Phys. Soc. Jpn. **53**, 4138 (1984); W. M. Zhang, W. M. Saslow, and M. Gabay, Phys. Rev. B **44**, 5129 (1991).

[11] T. Garel and J. M. Maillard, J. Phys. C **19**, L505 (1986).

[12] T. R. Welberry and R. Galbraith, J. Appl. Cryst. **6**, 87 (1973); I. G. Enting, J. Phys. C **10**, 1379 (1977).

[13] T. R. Welberry and R. Galbraith, J. Appl. Cryst. **8**, 636 (1975).

[14] T. Garel, J. C. Niel, H. Orland, and M. Schick, J. Phys. A **24**,

1245 (1991).

[15]I. G. Enting, J. Phys. C **6**, 3473 (1973); R. J. Elliott and N. Marshall, Rev. Mod. Phys. **30**, 75 (1958).

[16]J. Villain and P. Bak, J. Phys. (France) **42**, 657 (1981). A general reference on the *ANNNI* model is W. Selke, Phys. Rep. **170**, 213 (1988). In the specific context of microemulsions, the reader is referred to G. Gompper and M. Schick, Phys. Rev. B **41**, 9148 (1990).

[17]G. N. Hassold and D. J. Srolovitz, Phys. Rev. B **37**, 3467 (1988).

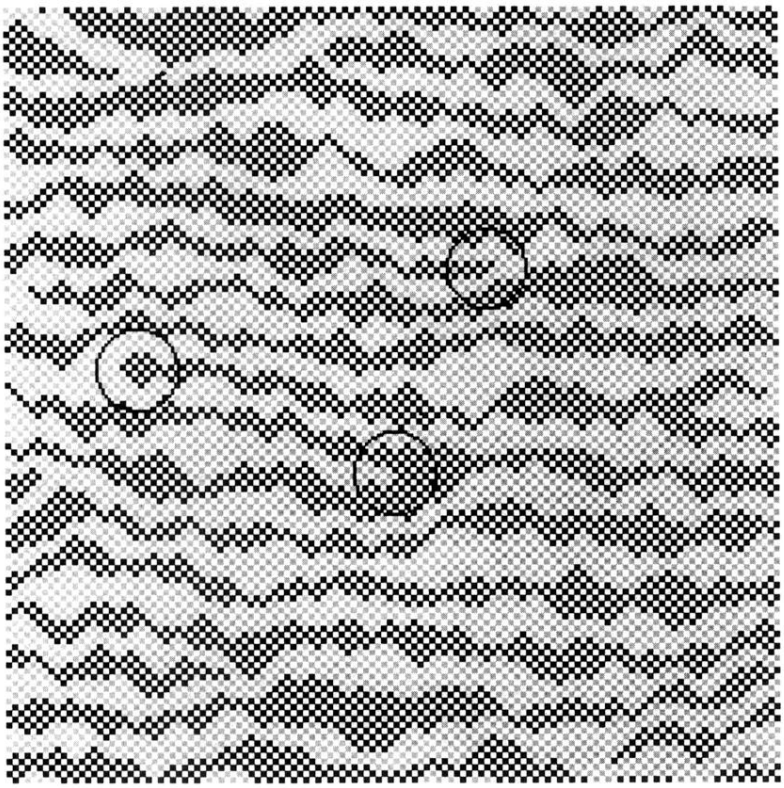

FIG. 5. Snapshot of a (64a*64b) part of the lattice after 256 MCS. Spin $+1$ (-1) are in black (grey). Dislocationlike configurations are clearly visible (circles). Note that the transformation $J_1 \rightarrow -J_1$ and $S_{u,v} \rightarrow (-1)^{u+v} S_{u,v}$ has been used in order to make more apparent the ordered domains.